

Integrated photodiodes complement the VCSEL platform

Martin Grabherr, Philipp Gerlach, Roger King, Roland Jäger
Philips Technologie GmbH U-L-M photonics, Lise-Meitner-Str. 13, 89081 Ulm, Germany

ABSTRACT

Many VCSEL based applications require optical feedback of the emitted light. E.g. light output monitor functions in transceivers are used to compensate for thermally induced power variation, power degradation, or even breakdown of pixels if logic for redundancy is available. In this case integrated photodiodes offer less complex assembly compared to widely used hybrid solutions, e.g. known in LC-TOSA assemblies. Especially for chip-on-board (COB) assembly and array configurations, integrated monitor diodes offer a simple and compact power monitoring possibility. For 850 nm VCSELs the integrated photodiodes can be placed between substrate and bottom-DBR, on top of the top-DBR, or inbetween the layer sequence of one DBR. Integrated intra-cavity photodiodes offer superior characteristics in terms of reduced sensitivity for spontaneously emitted light [1] and thus are very well suited for power monitoring or even end-of-life (EOL) detection. We present an advanced device design for an intra-cavity photodiode and according performance data in comparison with competing approaches.

Keywords: VCSEL, power monitoring, integrated photodiode

INTRODUCTION

Output power variation of VCSELs is due to temperature dependence of threshold current and slope efficiency, but also due to degradation over life time. In order to compensate for the power variation, or even detection of EOL criteria that enable redundant system designs, power monitoring of the output is crucial for many applications that rely on fixed optical power levels. Whereas the general temperature dependence of VCSELs is mostly given by material properties and requires compensation by closed loop power control, degradation behavior over lifetime has been improved significantly by enhanced device design and manufacturing techniques [2,3]. The random failure rates, excluding ESD related failures, have been reduced to less than 10 FIT [3]. Anyway, appropriate EOL detection would enable simplified redundant system design.

In general, output power of a VCSEL can be monitored by detecting the light extra cavity on either side of the resonator, or intra cavity by integrating a photodiode structure into the cavity design. Fig. 1 illustrates these three main options.

The most simple approach is making use of light emitted from the top side of the VCSEL and reflected back from an optical plane in a certain distance onto a separate photodiode chip adjacent to the VCSEL. The integrated extra cavity approach can be realized by photodiodes grown on top of the VCSEL or between the substrate and the cavity and adding the according electrodes to the chip design.

In the following we focus on 3 different approaches for power monitoring:

- 1: Standard external hybrid monitor diode, making use of the reflection of output power from a glass window cap of the package
- 2: Integrated monitor photodiode between substrate and bottom DBR (extra cavity)
- 3: Integrated monitor photodiode intra cavity in the n-doped bottom DBR

As an important performance criteria, the influence of spontaneous emission for the monitor signal will be investigated and discussed in terms of power tracking performance and EOL criteria.

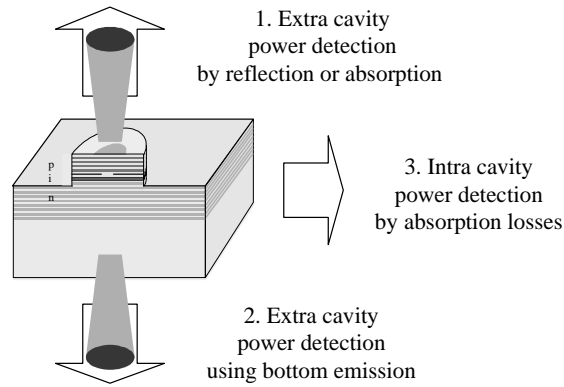


Fig. 1: Three main options to implement power monitoring functions:

- 1) reflections from top-emission at external optical planes or partial absorption when transmitting light through an integrated PD on top of the n-DBR
- 2) detection of the small light portion emitted through the high reflective mirror by an integrated monitor diode below the VCSEL cavity
- 3) intra cavity absorption by an integrated photodiode

VCSEL DESIGN

All devices under investigation are based on 850 nm oxide confined VCSELs. As a reference for the integrated approaches, a typical configuration of a top-emitting VCSEL on a large area Si-photodiode is used, as depicted in Fig. 2. The reflection of the emitted power at the flat glass of e.g. a cap of a TO can is used for power monitoring.

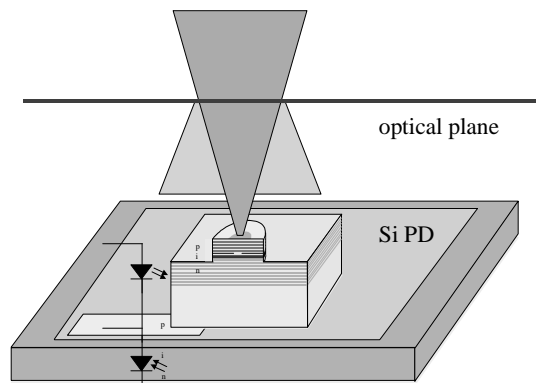


Fig. 2: Typical approach for power monitoring using the optical plane of, e.g. the reflections from a glass window of a cap of a TO can. The photodiode can be placed below or besides the VCSEL chip. Electrical connection is done by die attach and/or wire bonding.

We have investigated two different designs for the integration of a photodiode. In the first approach a regular VCSEL structure has been grown on top of a pin photodiode. A schematic drawing is given in Fig 3 (left side). The light which is emitted from the cavity to the bottom side is absorbed by a 2 μm thick GaAs layer. The PD area is laterally not constricted. The photodiode anode is built by a 3 μm thick layer, contacted from the top side by a via and shorted to the VCSEL cathode. Thus the device can be operated as a three terminal device.

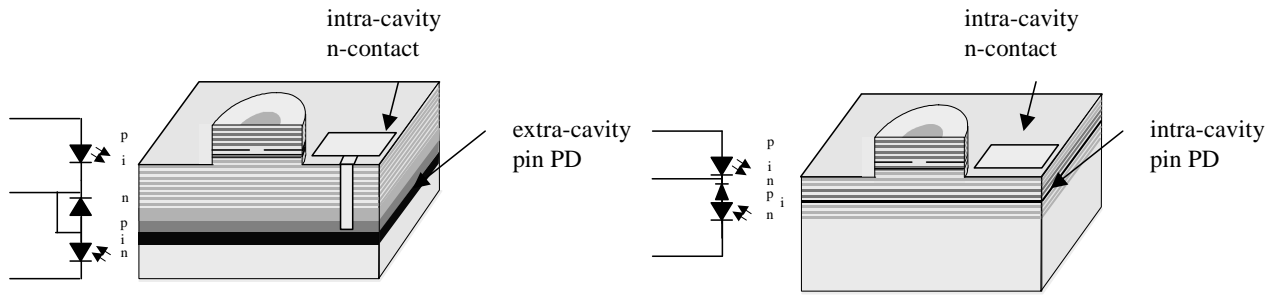


Fig. 3: LEFT: VCSEL with integrated photodiode between the bottom DBR and the substrate. The electrical connection of VCSEL cathode and PD anode is done by an intra cavity n-contact of the VCSEL and a via contact to the 3 μm thick p-doped layer of the PD and an electroplated gold pillar connecting both electrodes. The absorption layer consists of 2 μm thick nominally undoped GaAs. RIGHT: VCSEL with integrated intra-cavity photodiode. The bottom DBR consists of 3 areas, starting below the quantum wells with n-doped layers, changing to p-doped layers followed by a GaAs absorption layer of about 100 nm thickness placed around the antinode of the standing wave pattern. The pin-structure of the PD is finished by further n-doped DBR layer pairs. The intra-cavity VCSEL n-contact serves also as PD anode, as the pn-junction between VCSEL cathode and PD anode is driven in forward direction and thus the PD anode contact can be skipped.

A novel approach is placing the PD inside the cavity without additional contact or spacer layer, actually integrated into the bottom DBR which now consists of a first part of 16 n-DBR layer pairs and 2 p-doped DBR pairs followed by the 100 nm thick absorbing GaAs layer, which is placed symmetrically around an antinode of the standing wave pattern in order to get maximum responsivity and maximum contrast of stimulated versus spontaneous emission. The bottom reflector is completed by additional 22 pairs of n-doped DBR layer pairs. The intra-cavity contact in the central n-doped DBR part is used as both, VCSEL cathode and monitor anode. The additional pn-junction between VCSEL cathode and PD anode is not shortened, but driven in forward direction and thus just adding an additional voltage drop to the monitor diode.

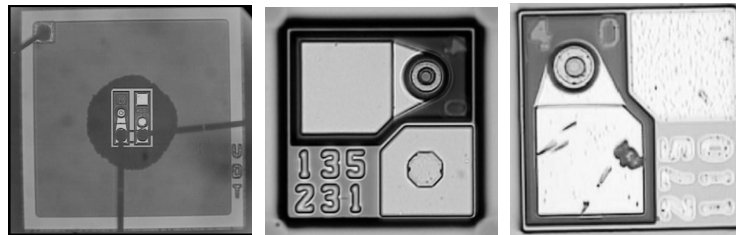


Fig. 4: LEFT: VCSEL chip on top of a 1.25x1.25 mm² silicon photodiode chip. CENTER: 4 terminal design of the integrated external cavity photodiode. In the lower right corner, the intra-cavity n-contact and the via connection to the PD anode can be seen. RIGHT: 3 terminal design of the intra-cavity photodiode.

In Fig. 4 the according pictures of the 3 different approaches are shown. The left side is showing the 1.25x1.25mm² large silicon photodiode carrying a VCSEL chip in the center pad. In this case the VCSEL anode, VCSEL cathode, and PD anode are connected by wire bonds. The central picture shows the top side of the VCSEL with integrated extra-cavity PD. In the lower right corner of the picture VCSEL cathode and PD anode pad is seen, the hexagonal structure in the center of the pad is caused by the via connection to the PD anode. The picture in right side of Fig. 4 is taken from a VCSEL with integrated intra-cavity photodiode.

LIGHT-CURRENT-VOLTAGE AND MONITOR CURRENT VS. TEMPERATURE

The cw light-current-voltage (LIV) output characteristics at -30 , $+25$, and $+90^\circ\text{C}$ of a free running VCSEL with 5 μm active diameter are shown in the left part of Fig. 5. The right side of Fig. 5 illustrates the typical temperature dependence of the threshold current and the slope efficiency. In this case the threshold current minimum is designed

around 10°C and increases parabolically with temperature, the slope efficiency is declining in first approximation linearly with temperature.

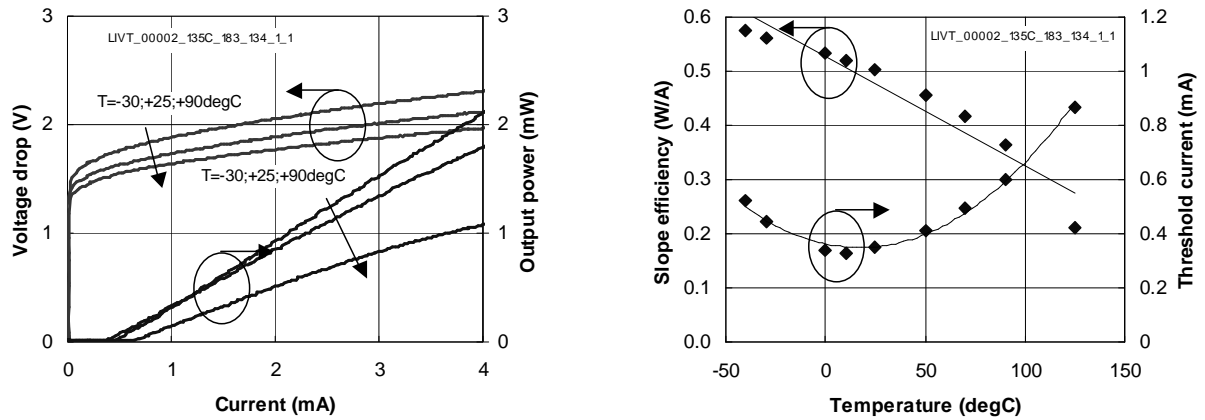


Fig. 5: LEFT: LIV output characteristics at -30°C, 25°C, and 90°C, of a 5 μm aperture VCSEL without monitor function. RIGHT: Typical temperature dependence of threshold current (approximately parabolic) and slope efficiency (approximately linearly decreasing).

The left part of Fig. 6 depicts the LIV curves at -10, +30, and +80°C ambient temperature of a 14 μm oxide aperture VCSEL. The VCSEL is placed on top of a silicon photodiode and mounted in a TO46 package with flat window cap, having a 50% reflection coating. The according monitor current is given in the right graph of Fig. 6. The upper part represents the monitor current according to the output power plotted in the lower part. The monitor current versus laser current curves show significant positive curvature, which is due to the dependence of the reflected and absorbed power to the farfield pattern of the VCSEL. The effect of increasing monitor current by spontaneous emission is negligible.

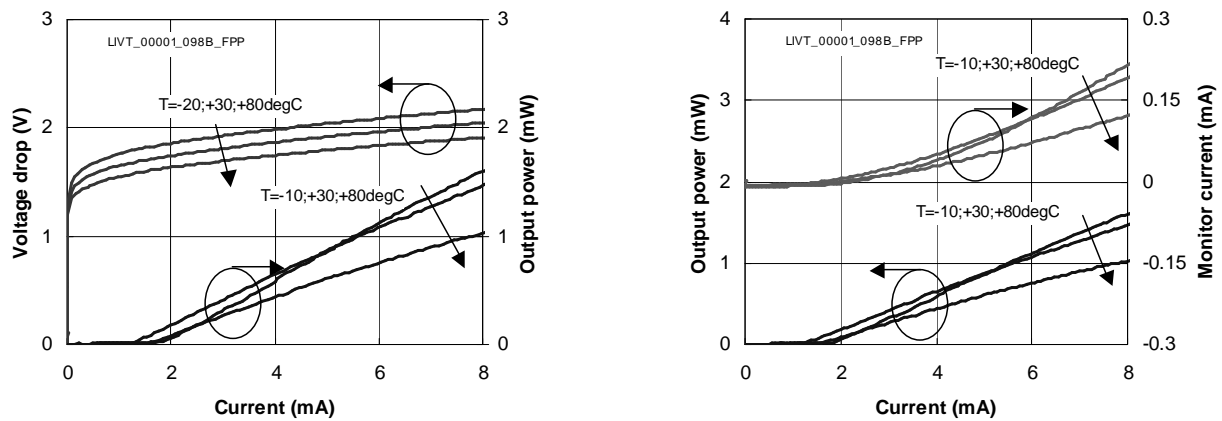


Fig. 6: LEFT: LIV output characteristics at -10°C, 30°C, and 80°C, of a 14 μm VCSEL, placed hybridly on a silicon photodiode. RIGHT: In the lower part, the LI characteristics are plotted again as reference, in the upper part the monitor current as a function of laser current is plotted. The influence of spontaneous emission is negligible for the hybrid solution, the non-linearity is due to the changing farfield pattern with laser current.

The cw LIV characteristics of the VCSEL with integrated extra-cavity PD is presented in the left part of Fig. 7. The output power level at operation conditions is designed to be comparable to the hybrid solution, including the reflection losses. In the right graph, the monitor current versus laser current is shown, again in comparison with the output power characteristics. The monitor current is growing linearly with increasing output power, but the sensitivity (represented by the slope of monitor current versus laser current) of the detection is even stronger for the spontaneous emission below threshold current.

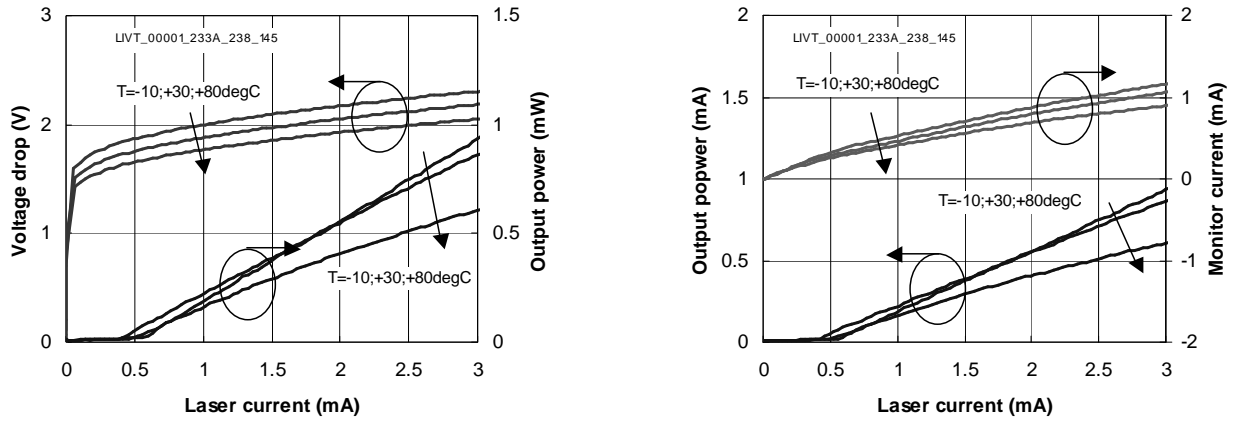


Fig. 7: LEFT: LIV output characteristics at -10°C , 30°C , and 80°C , of a $5\ \mu\text{m}$ VCSEL with integrated extra cavity monitor photodiode. RIGHT: In the lower part, the LI characteristics are plotted again as reference, in the upper part the monitor current as a function of laser current is plotted. As this design is strongly sensitive on spontaneous emission, the monitor current is increasing more strongly with laser current below laser threshold compared to lasing condition.

The VCSEL with integrated intra-cavity photodiode shows almost identical LIV performance compared to the previous extra-cavity design as can be seen in Fig. 8 left side. Only the spectral mismatch of resonance wavelength and gain peak at room temperature is smaller, thus the threshold current minimum is achieved at significantly lower temperatures. The monitor current, depicted in the upper part of Fig. 8, right side, is nicely linearly growing with laser current and the contribution of the spontaneous emission to the monitor current is strongly reduced.

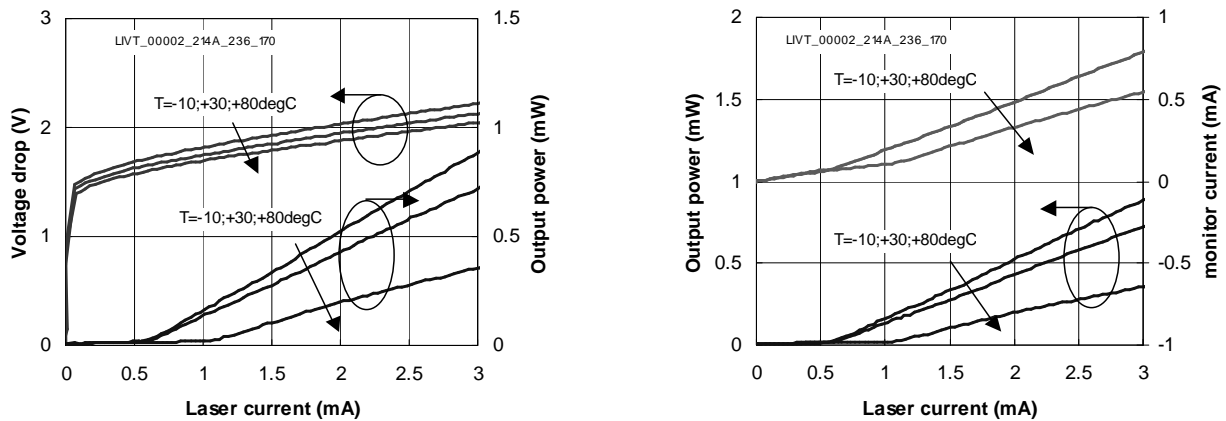


Fig. 8: LEFT: LIV output characteristics at -10°C , 30°C , and 80°C of a $5\ \mu\text{m}$ VCSEL with integrated intra-cavity monitor photodiode. RIGHT: In the lower part, the LI characteristics are plotted again as reference, in the upper part the monitor current as a function of laser current is plotted. The monitor current is increasing linearly with the laser current and the influence of the spontaneous emission is strongly reduced.

MONITOR VS. OUTPUT AND TRACKING ERROR

The basic differences in performance between the three approaches is clearly seen when plotting the monitor current versus laser current. Representing the hybrid configuration, Fig. 9 is showing negligible influence of spontaneous emission to the monitor signal as no offset in the monitor current is observed. The monitor current is slightly dependent on temperature and does show a significant positive curvature due to the already mentioned power and temperature dependent farfield characteristics.

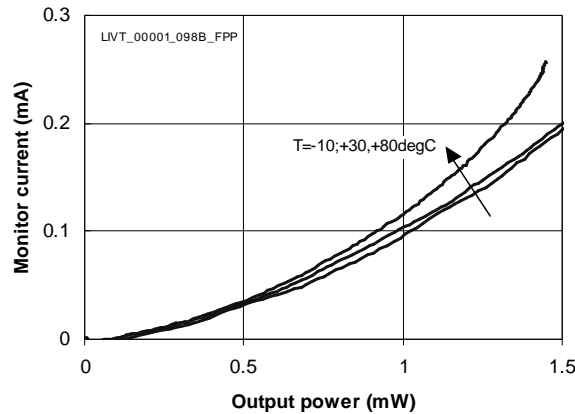


Fig. 9: Monitor current versus output power for the VCSEL with external, hybrid monitor function. The non-linearity is due to the change in farfield characteristics and the according influence on the reflection at the external optical plane. Spontaneous emission does not contribute to the monitor signal.

The left part of Fig. 10 relates to the VCSEL with integrated extra-cavity photodiode. A significant offset in monitor current which is due to the temperature dependent threshold current is observed. The monitor current is increasing linearly with output power and only a weak dependence on temperature is present. For the on-state in data transmission of e.g. 0.5 mW the offset amounts to about 40 % of the monitor signal and even worse, in the off-state at e.g. 0.12 mW the offset is even dominating. As the offset is due to contribution of spontaneous emission and the threshold current is changing with temperature and over lifetime of the device, this scenario is disadvantageous for a closed loop power control.

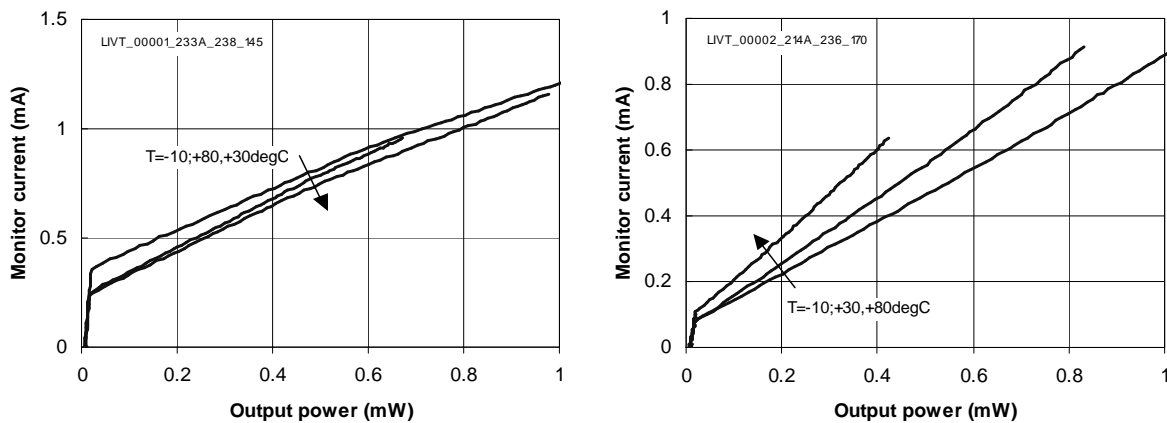


Fig. 10: LEFT: Monitor current versus output power for the VCSEL with integrated extra cavity monitor diode. The offset in monitor current is due to the detection of spontaneous emission and accounts for a large part of the total monitor current. RIGHT: Monitor current versus output power for the VCSEL with integrated intra cavity monitor diode. The offset in monitor current is significantly smaller. The monitor signal versus output power is perfectly linear. The strong temperature dependence of the corresponding responsivity monitor current versus output power is due to the temperature dependent absorption coefficient of the absorbing layer.

The device with integrated intra-cavity photodiode behaves very different as can be seen in the right part of Fig. 10. The spontaneous emission, effecting the offset in the monitor current, is not contributing significantly and the monitor current is linearly growing with output power. Even in the off-state at 0.12 mW the contribution of stimulated emission to the monitor signal is at least at the same level compared to the spontaneous emission. However, a strong dependence of the absorption coefficient on temperature is observed, which results in the different slopes for the temperatures of -10, +30, and +80°C. This behaviour is due to the short absorption length of only 100 nm and the emission wavelength

which is close to the fundamental absorption limit of the GaAs layer and thus turns out to be very sensitive on wavelength variation.

As a result, Fig. 11 and Fig 12 show the tracking errors for all 4 devices. Tracking error for the devices with monitor photodiode is defined as the deviation of output power compared to the output power at 25°C, given a constant monitor current. For the free running VCSEL, tracking error is defined as the power variation at constant laser current, again referred to the conditions at 25°C. According graphs for the free running VCSEL are depicted in Fig 11, left side. In the on-state (dotted line), the free running VCSEL is suffering from reduced slope efficiency in combination with increased threshold current at high temperature, whereas at low temperature, increased slope efficiency partly compensates for the increase in threshold current. In the off state (dashed line) the tracking error is dominated by the temperature dependence of the threshold current and the graph shows a very strong parabola and a -3 dB power drop at 80°C. When using the external silicon photodiode as monitor, the tracking error remains within +/-10 % over the entire temperature range of -10 to 80°C and for all power levels, as can be seen in the right part of Fig. 11. The residual oscillations are due to the increments of the measurement. This result represents an almost ideal tracking behavior.

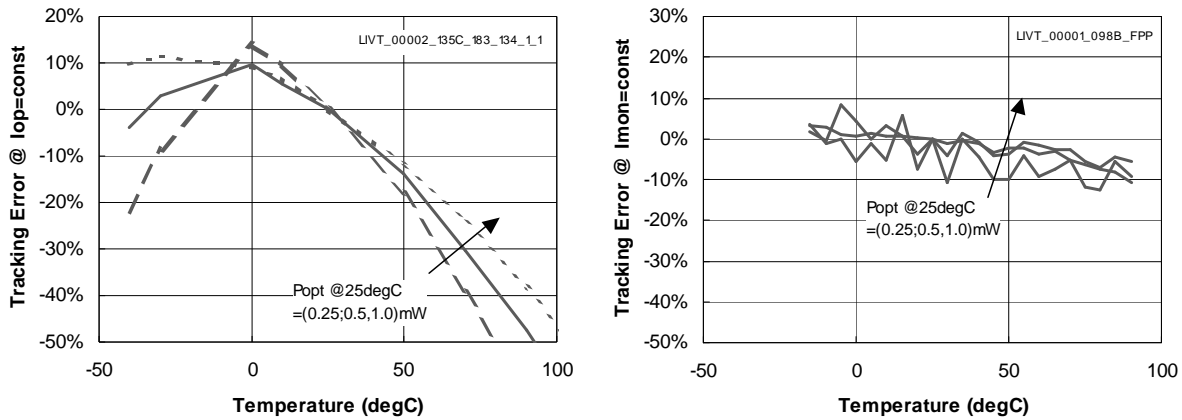


Fig. 11: LEFT: Tracking error for the free running VCSEL. RIGHT: Tracking error of the VCSEL with external, hybrid monitor function. Both graphs are referenced to the output power levels at 25°C

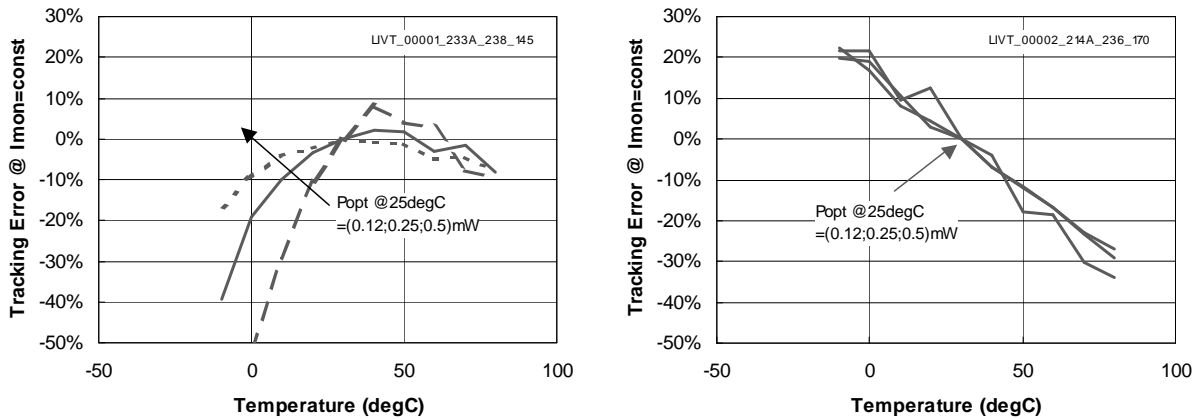


Fig. 12: LEFT: Tracking error for the VCSEL with integrated extra-cavity photodiode. Especially for low output powers, the spontaneous emission causes significant deviation. RIGHT: Tracking error of the VCSEL with integrated intra-cavity photodiode. Although the deviation is large, the tracking error is independent on power level and linear with temperature. By reducing the temperature dependence of the absorption coefficient, the tracking error can be independent also on temperature. Both graphs are referenced to the output power levels at 25°C

The tracking error over temperature for the VCSEL with integrated extra-cavity photodiode is plotted in the left part of Fig. 12. In the on-state the tracking error is acceptable with a maximum of -20% at -10°C . But in the off-state, the tracking error reaches -3 dB already at 0°C because of the strong contribution of the spontaneous emission to the monitor signal. Actually, the monitor signal indicates already lasing although the VCSEL operation is still below threshold due to the strong sensitivity of the photodiode on spontaneous emission. The right part of Fig. 12 is showing the according tracking error for the VCSEL with integrated intra-cavity photodiode. The three curves for the different power levels are almost identical, which means that the on- and off-state of the VCSEL can be controlled by the same driver concept in terms of temperature compensation. The strong temperature dependence of the tracking error is due to the spectral sensitivity at the fundamental absorption limit of the 100 nm thick GaAs layer and can be improved by optimized material composition.

IMPACT OF DEGRADATION ON POWER MONITORING

Besides temperature dependence of the output characteristics and tracking error at different power levels, degradation behavior of the power monitoring is crucial for the system design. Focussing on the integrated photodiodes, the VCSEL with intra-cavity photodiode has been selected for this evaluation, as the typical degradation mechanism is causing an increase in threshold current and a decrease in slope efficiency. Obviously, the change in threshold current will result in even worse tracking behaviour for the extra-cavity approach.

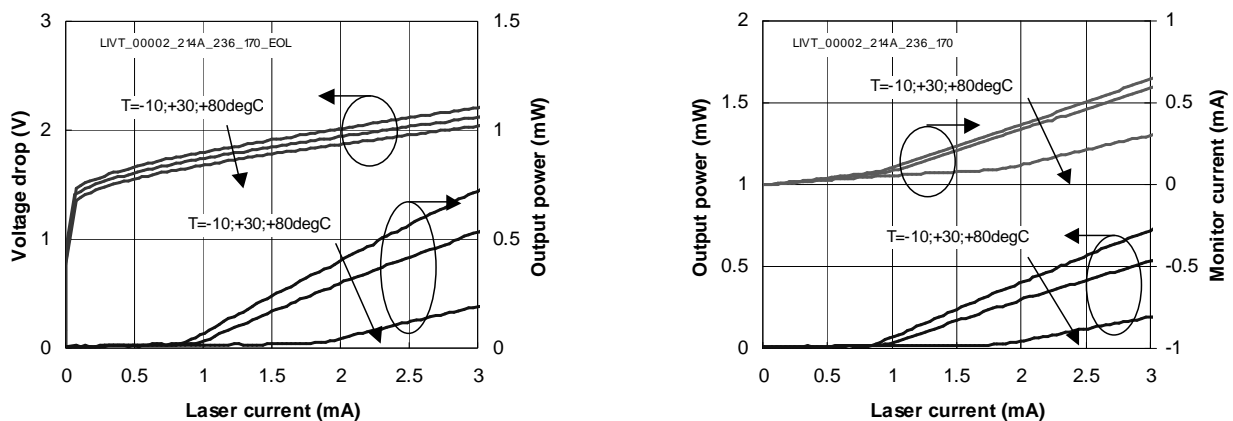


Fig. 13: LEFT: LIV output characteristics at -10°C , 30°C , and 80°C , of a $5\ \mu\text{m}$ VCSEL with integrated intra-cavity monitor photodiode after aging. RIGHT: In the lower part, the LI characteristics are plotted again as reference, in the upper part the monitor current as a function of laser current is plotted. Please compare to Fig. 8.

Comparing the left part of Fig. 8 (no aging) with the left part of Fig. 13 (after aging), the main changes are an increase in threshold current by a factor of about 2. The changes in IV characteristics and slope efficiency are marginal. In the right part of Fig. 13 the monitor current (top) and output power (bottom) versus laser current is plotted. The shift of the threshold currents is of course translated to the monitor current, but still the monitor signal is nicely linear with the laser current. As a result, in Fig. 14 (left side) you can see that the monitor current versus output power graph did not change significantly, just the power levels that are reached are reduced compared to Fig. 10, right side. The tracking error versus temperature after aging of the device thus remains the same as can be seen in Fig 14, right side. There is still no dependence on power level and the temperature dependence is still linear.

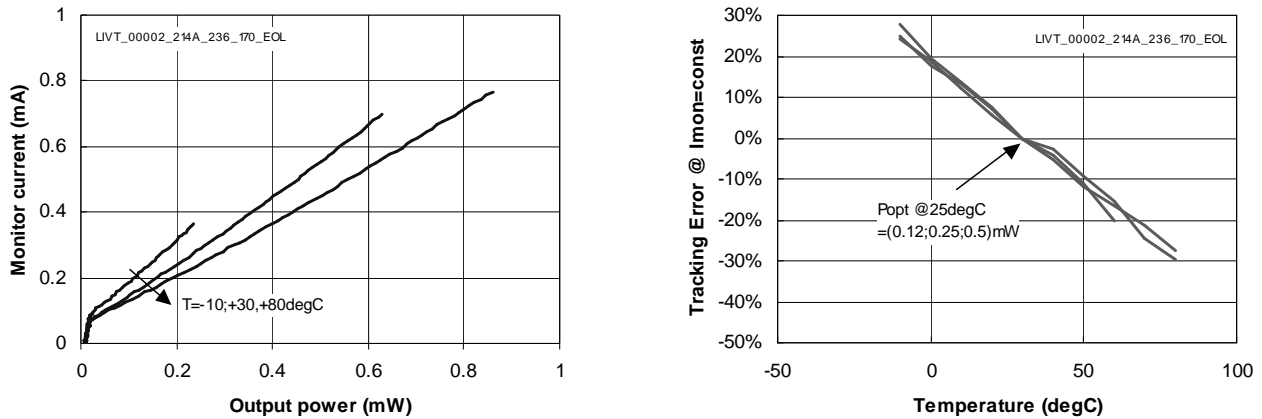


Fig. 14: LEFT: Monitor current versus output power for the VCSEL with integrated intra-cavity monitor diode after aging. Compared to Fig. 10 (right side), no change in monitoring performance can be seen. RIGHT: Tracking error of the VCSEL with integrated intra-cavity photodiode after aging. No change in tracking error performance can be seen over the life time (compare with Fig. 12 (right side)).

CONCLUSION

Looking at the power monitoring performance, the hybrid solution with external silicon photodiode and an optical reflection at external optical plane provides best performance. Due to the geometrical conditions, contribution of spontaneous emission is negligible. Thus the hybrid approach is rather independent on temperature and power levels. The artifacts caused by farfield pattern changes with power and temperature are of minor importance. Of course, the hybrid approach does not qualify for chip on board designs and monolithic array configurations

The VCSEL with integrated extra-cavity photodiode suffers from strong contribution of the spontaneous emission to the monitor signal. As the threshold current is dependent on temperature and aging, especially low power levels are causing significant tracking errors. Even in comparison with the free running VCSEL, power stabilization is not improved.

For the VCSEL with integrated intra-cavity photodiode, power monitoring and thus tracking is almost independent from spontaneous emission and therefore this approach is very promising for the power monitoring and closed loop power control in integrated systems. Especially the identical tracking behavior for all power levels is very attractive for optimizing data transmission dynamics. The observed strong temperature dependence is due to the implemented thin GaAs absorption layer and the according spectral sensitivity. Improvements can be expected by changing the material composition of the absorbing layer slightly towards smaller band gap material. The excellent characteristics of the integrated intra-cavity photodiode are not changing during aging and allow for identical control mechanism over the entire lifetime of the device. In addition to output power control, the stable monitoring characteristics also allow for EOL detection by verifying the monitor current at certain boundary conditions, as contribution from spontaneous emission can not cause false interpretation.

SUMMARY

We have compared one hybrid and two integrated approaches for power monitoring of VCSELs and with a free running VCSEL. For chip-on-board assembly and array configurations, VCSELs with integrated intra-cavity photodiodes are best suited for power monitoring, as they provide a compact and excellent power monitoring without external components. Their independence on contributions from spontaneous emission offers promising power control over temperature and lifetime. In order to reduce the residual temperature dependence, material optimization of the absorbing layer is required.

REFERENCES

- [1] Lim, S. F. et al.: "Intracavity Quantum-Well Photodetection of a Vertical-Cavity Surface Emitting Laser", Proc. Int. S.C.-Laser Conf. Haifa-Israel, 183-184 (1996).
- [2] D. Wiedenmann et al., "High volume production of single-mode VCSELs", Proc. SPIE 6132, 613202-1 - 613202-12 (2006).
- [3] J. Guenther et al., "Developments at Finisar AOC", Proc. SPIE 6908, 690805-01 - 690805-8 (2008).